A R C H I V E S O F M E T A L L U R G Y A N D M A T E R I A L S
Volume 53 2008 Issue 1

W. RATUSZEK*, J. KOWALSKA*, A. BUNSCH*, M. RUMIŃSKI*, A. ZIELIŃSKA-LIPIEC*

DEVELOPMENT OF DEFORMATION TEXTURE OF AUSTENITIC STEEL WIRES

ROZWÓJ TEKSTURY ODKSZTAŁCENIA W DRUTACH ZE STALI AUSTENITYCZNEJ

The present work refers to a development of texture and microstructure in wires of AISI 302 austenitic steel subjected to multistage drawing process. The analysis of texture focused on pole figures, orientation distribution functions (ODFs) and inverse pole figures. The texture measurements were conducted on the sections parallel to the wire axis. The microstructure was observed using optical and transmission electron microscopes.

The martensitic transformation ($\gamma \rightarrow \alpha'$) was induced by plastic deformation in the whole range of deformations. The texture development of both phases i.e. austenite and martensite was analysed. The texture components were characterized by crystallographic direction parallel to the axes of the wires. The <111> and <001> orientations were main components of the austenite texture, while, in the martensite they were <110> and <021> ones. The equiaxial grains of austenite containing annealing twins were observed within the microstructure in the initial state. During the deformation process the shape of austenite grains changed into long slim bands parallel to the drawing direction. Many shear bands were observed in the microstructure at large deformations. The martensite, which formed as a result of deformation induced transformation ($\gamma \rightarrow \alpha'$), influenced properties of the steel. The hardening of the material resulted from a significant increase of the volume fraction of the α'-martensite in the structure of the steel.

Keywords: austenitic steel, wires, texture, microstructure, martensite transformation

Prezentowana praca dotyczy rozwoju tekstury i mikrostruktury austenitycznych drutów ze stali AISI 302 poddanych procesowi wielostopniowego ciągnienia. Analizę tekstur przeprowadzono w oparciu o figury biegunowe, funkcję rozkładu orientacji FRO oraz odwrotne figury biegunowe. Pomiaru dokonano na przekroju podłużnym drutu. Mikrostrukturę obserwowano stosując mikroskop optyczny i transmisyjny mikroskop elektronowy.

Odkształcenie plastyczne indukowało przemianę martenzytyczną $\gamma \rightarrow \alpha'$ w całym zakresie odkształcenia. Obserwowano rozwój tekstury zarówno austenitu jak i martenzytu. W teksturze austenitu dominowały orientacje <111> i <001> równoległe do osi drutu. Głównymi składowymi tekstury odkształcenia martenzytu były <110> i <021>. W stanie wyjściowym w mikrostrukturze obserwowano równoosiowe ziarna austenitu z bliźniakami wyżarzania. Po odkształceniu ziarna przybierały postać długich cienkich pasm równoległych do kierunku ciągnienia. W mikrostrukturze materiału obserwowano liczne pasma ścinania. Martenzyt powstały w wyniku przemiany $\gamma \rightarrow \alpha'$ indukowanej odkształceniem wywierał istotny wpływ na własności stali. Martenzyt przy znacznym udziale objętościowym w strukturze prowadził do umocnienia materiału.

1. Introduction

Corrosion resistant austenitic steels contain chromium (17–25%), nickel (8–39%) and also additions of carbon (up to 0.1%), nitrogen, manganese, molybdenum and silicon [1]. Typical example of such steels has long been known as 18-8 stainless steel. It has found a wide applications and most of the currently used grades of austenitic steels have the chemical composition which is the modified composition of the original steel with 18% of Cr and 8% of Ni. In many works, among others these of Long, Delong, or Schaeffler [2], the influence of the alloying elements on the stability of austenite and ferrite was investigated. Hull [3] modified Scheafflers diagram to estimate the volume fraction of the ferrite and austenite in the steel based on its chemical composition and suggested that the fully austenitic structure can be obtained only if $R_{Ni}>(R_{Cr}-8)$.

Annealed austenitic steels have low yield strength $R_{0.2}$ = 200 – 250 MPa which is similar to the yield strength of carbon steels. Their tensile strength lies within the range of 520 to 760 MPa. The increase of the

* DEPARTMENT OF PHYSICAL AND POWDER METALLURGY, AGH – UNIVERSITY OF SCIENCE AND TECHNOLOGY, 30-059 KRAKÓW, AV. MICKIEWICZA 30, POLAND

yield strength of these steels can be attained by cold deformation. Particularly extremely high yield strength of 1200 MPa or even higher can be obtained in cold drawn wires [4].

The steel structure changes during deformation in dependence on its chemical composition, stacking fault energy (SFE), thermodynamical stability of its constituent phases as well as deformation conditions like temperature and strain. The martensitic transformation which may occur during cooling or cold deformation influences the structure of FCC steels [1, 5–17]. Stability of the austenite is characterised by $M_{d30/50}$ temperature (i.e. temperature at which at 30% deformation, 50% of its structure transforms into martensite). This temperature can be calculated based on the chemical composition of the steel [8–10]. Thomas and Henry [11] have carried out investigations of the austenitic steels to recognise the mechanisms of the plastic deformation and the dependence of microstructure changes on temperature and SFE. Their results for the deformation temperature lower than 0.5 melting point can be described as follows:

- For stable austenite and high SFE steels, dislocation glide operates as a main deformation mechanism.
- When austenite becomes unstable and SFE is low, apart from the dislocation glide, also glide of the partial dislocations, microtwining and phase transformations $\gamma \rightarrow \varepsilon$, $\gamma \rightarrow \alpha$ and $\gamma \rightarrow \varepsilon \rightarrow \alpha$ may take place as the deformation processes.

Deformation conditions and the operating deformation mechanisms influence the texture development of steels. In the case of austenitic steels, also phase stability which affects its final texture plays a significant role. Austenite texture according to previous investigation can be defined as a transition texture between so called metal and brass-type rolling texture. When martensite forms during the deformation process due to the strain-induced phase transformation it is also textured. Most of the authors have found that the crystallographic relations between the austenite and martensite textures have been best described by the Kurdjumov-Sachs or Nishyjama-Wasserman relationships [5–7, 18].

2. Material and experimental procedure

The cold-drawn wires of the austenitic AISI302 steel of chemical composition given in Table 1 were investigated in this work. The wires with 5.5 mm diameter were solution treated and again cold drawn in a multistage process to reduce the diameter to 1.59 mm. The deformation schedule is given in Table 2. After each stage of deformation a sample of the material was cut off the wire and taken for investigation.

The starting material and the samples from all subsequent deformation stages were investigated by means of diffraction methods. The measurements were performed on the longitudinal sections as shown in Fig. 1. Qualitative and quantitative phase analyses were carried out on HZG4 diffractometer using Fe Kα radiation of $\lambda_{K\alpha} = 0.1937$ nm. Texture measurements were done on Bruker D8 Advance diffractometer using Co Kα radiation of $\lambda_{K\alpha} = 0.17902$ nm.

Three incomplete pole figures – for each phase were recorded of; {111}γ, {200}γ, {220}γ planes for austenite and the {110}α, {200}α and {211}α for martensite and the orientation distribution functions (ODFs) were calculated for both phases.

The metallographic optical microscope Leica 3000N and transmission electron microscope JEM 200MX were used for microstructure observation. Mechanical properties were measured in Instron 1196 and 4502 tensile machines.

TABLE 1

The chemical composition of the AISI 302 steel [wt.%]

C	Cr	Ni	Mn	Mo	Si	P	S	N	Fe
0.094	17.62	7.75	0.89	0.42	0.7	0.026	0.003	0.03	balance

TABLE 2

The scheme of drawing AISI 302 steel wire and volume fraction of martensite

ϕ [mm]	5.5	4.35	3.56	2.98	2.46	2.15	1.98	1.9	1.81	1.7	1.59
$\varepsilon = \frac{\Delta S}{So} * 100\%$	0	37.4	58.1	70.6	80	84.7	87	88	89.1	90.4	91.6
% martensite	0	11.6	19.6	21.2	23.5	25.8	31.9	33.8	38.4	39.0	45.2

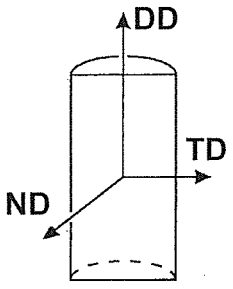

Fig. 1. Sample orientations – investigated wires cross-section: ND – normal direction, DD – drawing direction (wires axis), TD – transverse direction (of the cross section)

3. Results and discussion

The AISI 302 wires showed pure austenitic structure confirmed by the X-ray diffraction in which only (111)γ, (200)γ, (220)γ and (311)γ lines were present (Fig. 2a). The 110α, 200α, and 211α lines appeared in the diffraction patterns after 51.8% deformation. The quantitative phase analysis detected 28.5% of martensite in the wire structure at this deformation stage. In the solution treated samples only austenite diffraction lines were present again in the diffraction diagrams due to the reverse transformation $\alpha \rightarrow \gamma$ (Fig. 2b). With increasing deformation of the sample the following changes in diffraction diagrams were observed:

- austenite (111)γ lines became weaker while the (200)γ lines became stronger,
- new martensite lines appeared and their intensity increased,
- intensity of austenite lines decreased (Fig. 2b).

The difference in the relative intensity of the diffraction lines for both phases compared to the theoretical intensity for randomly oriented powder samples of austenite and martensite indicated that both phases were textured.

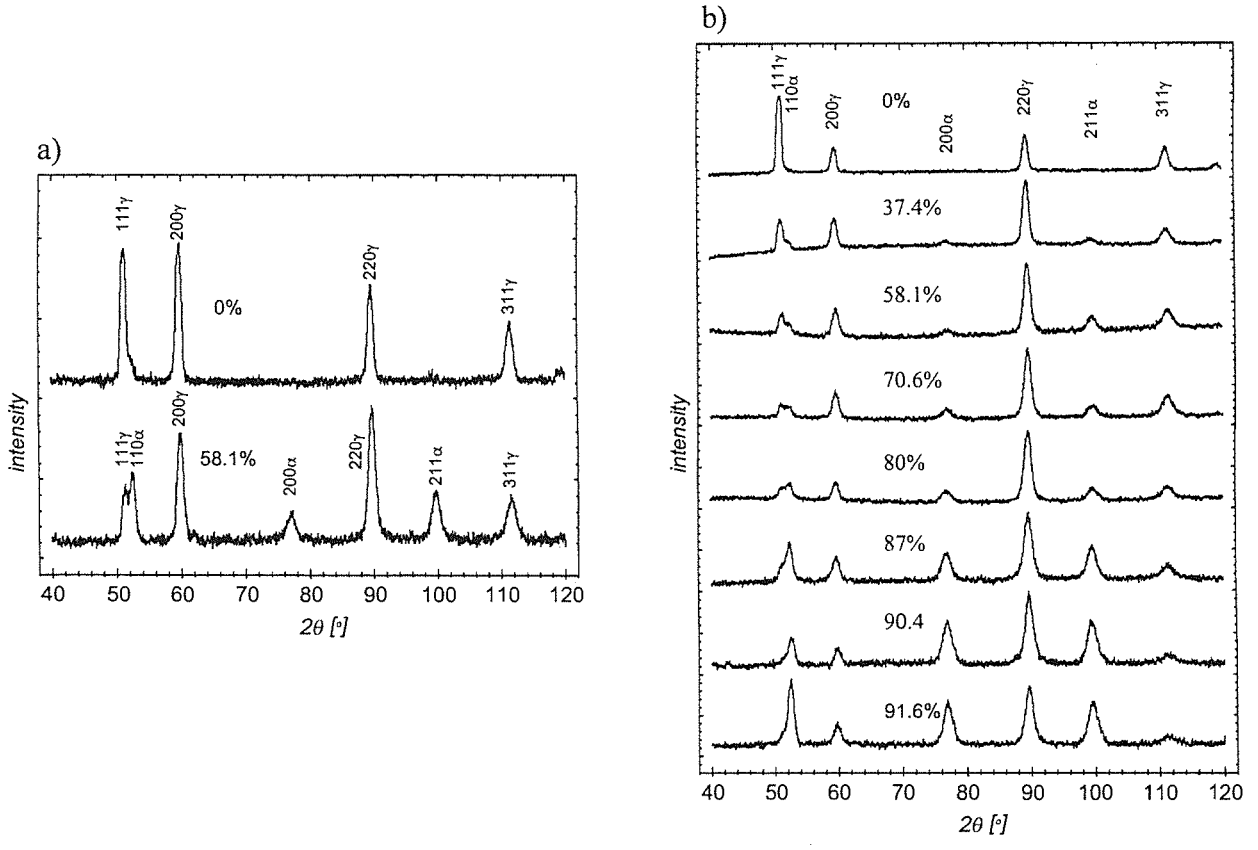

Fig. 2. The X-ray diffraction patterns of the AISI 302 steel: (a) in the initial state and after 58.1% of deformation, (b) after solution treatment and deformation in the range 37.4÷91.6%

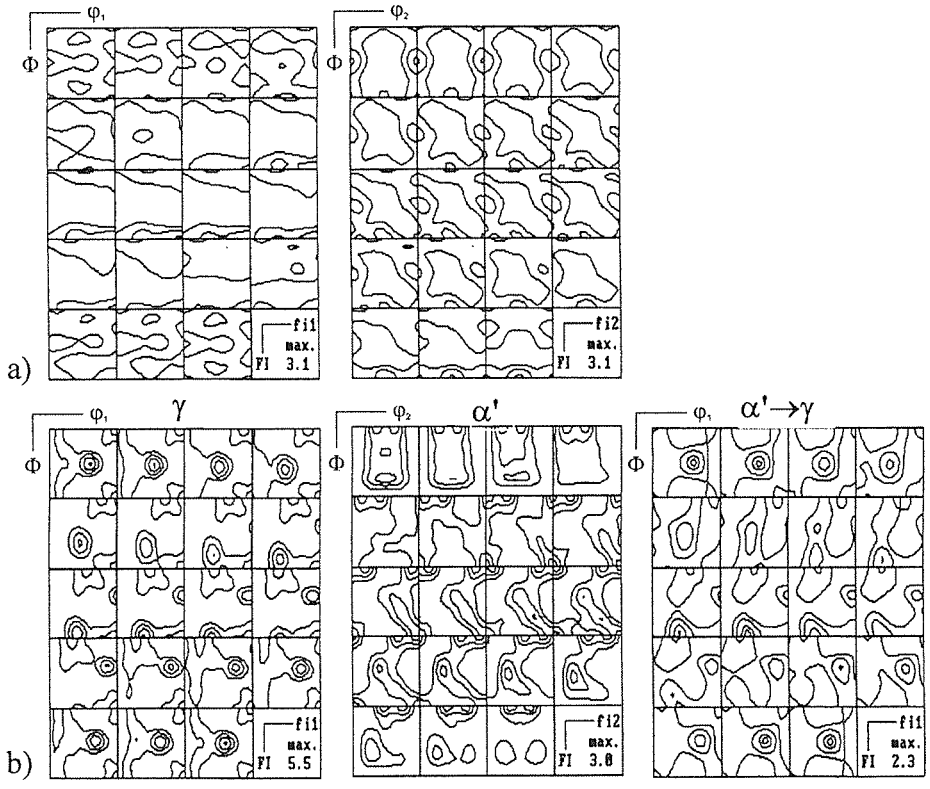

Fig. 3. Orientation distribution functions (ODF) of AISI 302 steel: (a) for the austenite in the initial state, (b) for the austenite (γ), martensite (α) and after transformation α′ → γ deformed 58.1%

Texture of austenite steel wires at the starting stage was very weak (Fig. 3a) and the Goss orientation was recognized as the strongest austenite texture component. Wires deformed to 58.1% contained textured austenite and martensite. The austenite had the fibre-type texture with the strongest {011}<111> orientation which belonged to the α<110> fibre. The orientations with <111> and <001> directions, which prevailed in the austenite grains were parallel to the wire axis. Apart from the austenite there was also 28.5% of martensite in which the strongest texture components were orientations for which <101> directions were parallel to the wire axis (Fig. 3b).

The solution treatment resulted in the weakening of the austenite texture, although its fibre character was retained (Fig. 4a). The {011}<111> orientation was still the major component in the austenite texture but the amount of the <001> component was very low. Martensite was not observed in the structure after solution annealing.

Subsequent deformation of the wires gave as a result changes in the austenite texture. During increasing deformation martensite was formed by the strain induced phase transformation and its texture was modified in the course of subsequent deformation stages. Two components the {hkl}<111> and {hkl}<001> in which <111> and <001> directions were parallel to the wire axes dominated in the texture of deformed austenite. The {011}<111> and {112}<111> orientations were the strongest among them. The martensite formed by strain induced transformation exhibited evident but weak texture. The major components in the martensite texture were those which had <120> and <110> directions parallel to the wire axes. With the deformation increasing over 70%, the intensity of the austenite texture was reduced. This can be explained by the transformation of austenite into martensite due to strain. The austenite {110}<112> and {112}<111> texture components disappeared and at the same time martensite with the two; {001}<110> and {211}<011> texture components was formed (Fig. 4). This observation is in good agreement with previous investigations [6, 16, 18 and 20], in which the authors reported the following relations between austenite and martensite texture components:

- {112}<110> component of the martensite texture was formed through the phase transformation from austenitic grains with Goss orientation {110}<001>,
- {332}<113> and {001}<110> martensite components appeared from parent austenite grains with {110}<112> orientation.

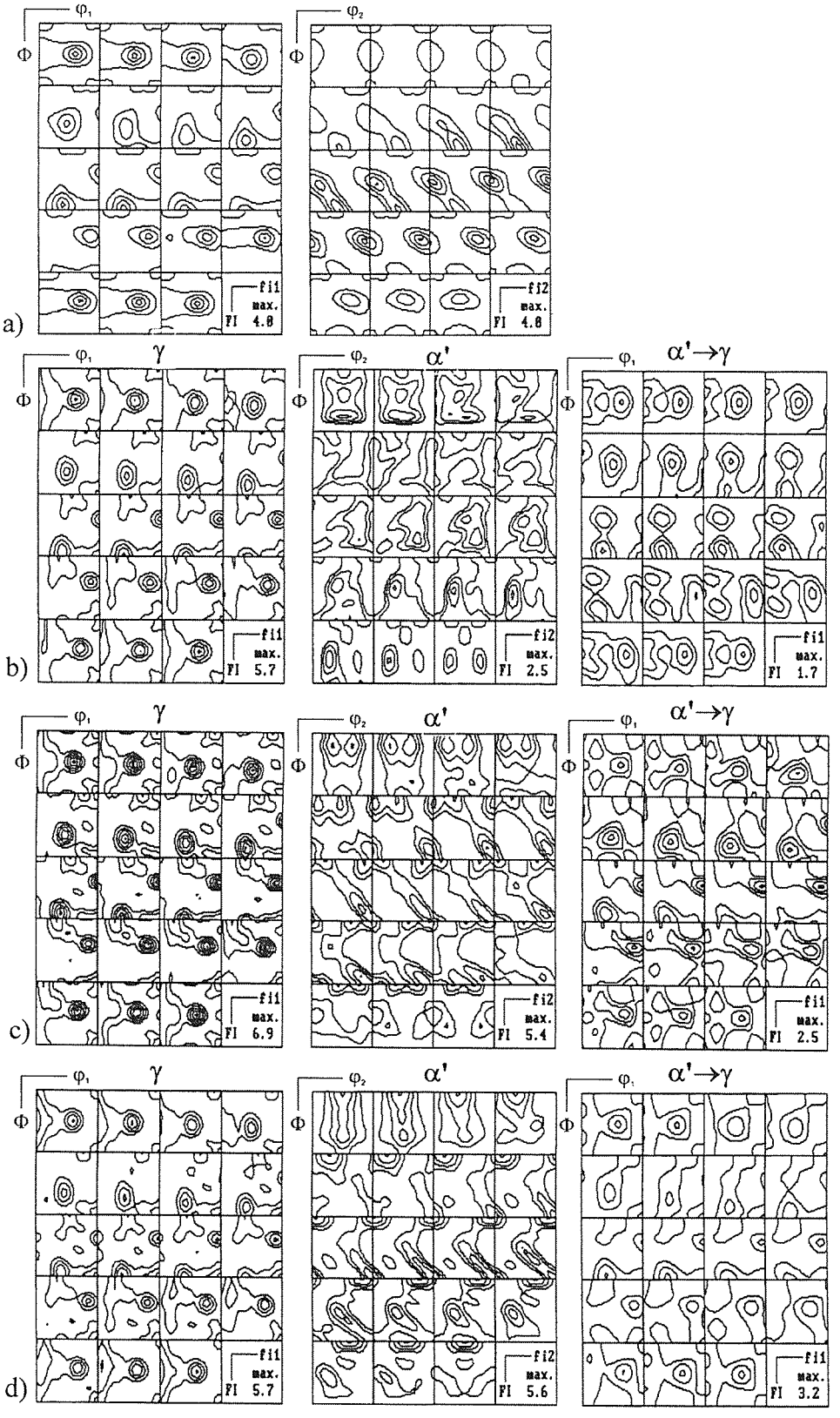

Fig. 4. Orientation distribution functions (ODF) of AISI 302 steel: (a) for the austenite after solution treatment, for the austenite (γ), martensite (α) and after transformation α′ → γ – (b) 37.4%, (c) 70.6%, (d) 91.6%

Martensite texture emerged from the austenite orientations which were contained in the α-fibre <110> ND as well as from the {112}<111> and {123}<111>orientations laying in its spread. With increasing deformation the martensite texture changed due to two simultaneous processes. One was the phase transformation of austenite into martensite and second was the martensite orientation changes during deformation of the wires. In other words: the martensite texture appeared in subsequent processes of martensite formation and its deformation which gives as a result the crystallographic lattice rotation. The texture of the martensite which was formed during strain induced deformation was weaker than the texture of the austenite matrix. This is a typical phenomenon for the structure obtained by the phase transformation which follows the crystallographic relation between the product and the parent phase [19].

Computer aided simulations were carried out to recognise mutual crystallographic relation between the austenite and martensite texture components. The ideal orientations corresponding to the main austenite texture components were transformed into theoretical martensite orientations assuming that those orientations were related with Kurdjumow-Sachs (K-S) relation. By comparing the results of such a simulation with the experimental martensite texture it was found that K-S relation described well the mutual relation of the α and γ texture components (Fig 3b and 4). Since the theoretical transformation was performed assuming all variant selections were equally, probable the obtained orientation distribution function (ODF) exhibited lower values than the experimental ones. The K-S relation was also reported by Ravi Kumar et al [6] as best describing the mutual orientation between austenite and martensite texture components in the metastable austenitic steels.

The yield strength ($R_{0.2}$) of the wires varied with the deformation degree. In the samples deformed more than 80%, local decrease of the yield strength was observed but this gave as a result the increase of the plasticity margin (Fig. 5). In that deformation range fast increase of the martensite volume fraction was observed in the structure. This led to the structure strengthening as a result of strain hardening. This process, probably responsible for variation of the yield strength at higher deformation, was precisely analysed in other work [12].

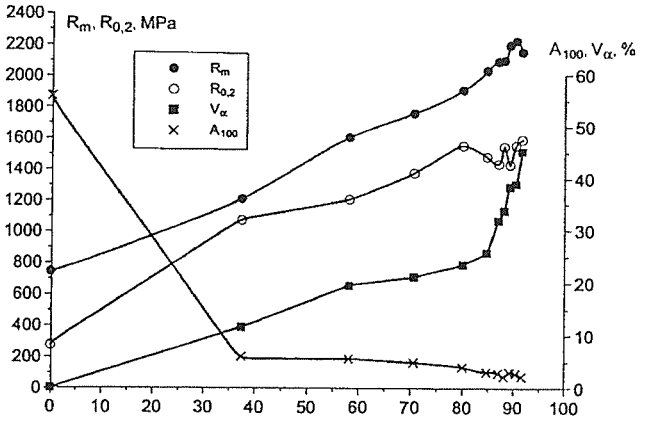

Fig. 5. Variation of mechanical properties and α-phase volume fraction as a function of the amount of deformation

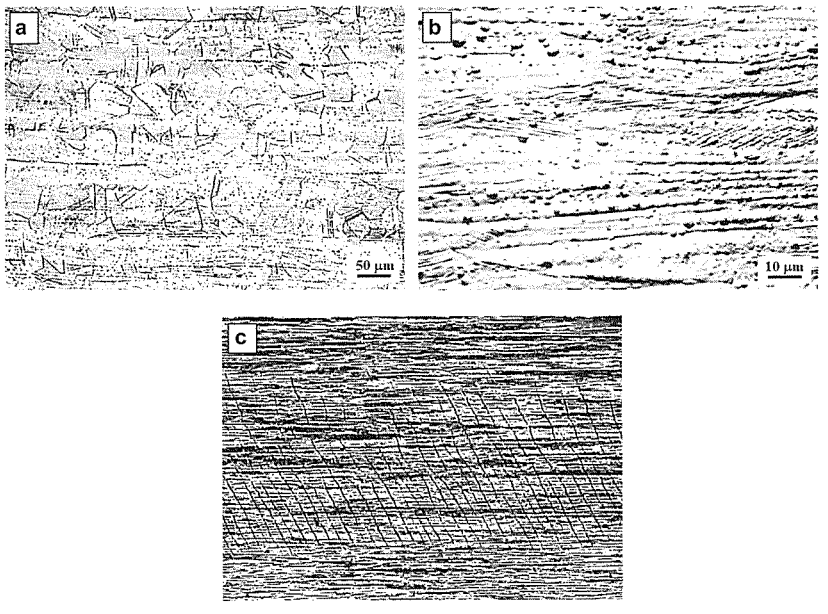

Fig. 6. Optical microstructure of the AISI 302 steel: (a) after solution treatment, (b) after 70.6% of deformation, (c) after 91.6% of deformation and annealing at 550° for 30 minutes

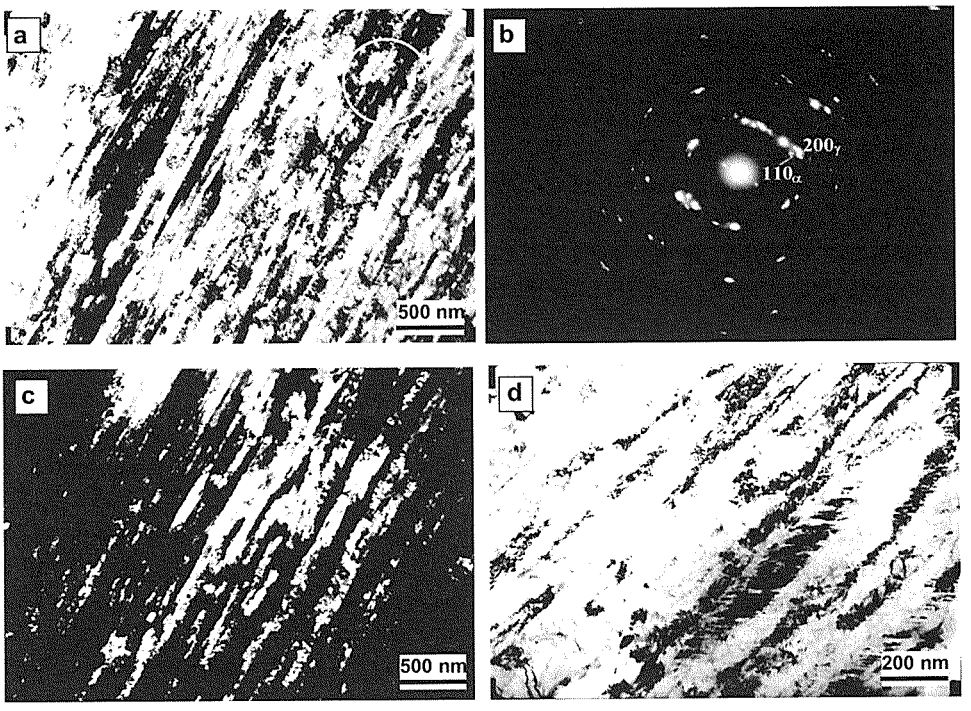

Fig. 7. TEM microstructure of the AISI 302 steel after 80% of deformation: (a) a band containing high amount of microareas of variable dislocation density, (b) SAED taken from the marked area, (c) darl field (DF) taken of the relation (011)α', (d) martensite areas inside a band of variable dislocation density

After solution treatment of the wires, equiaxial austenite grains with numerous recrystallisation twins were visible in the structure (Fig. 6a). When deformed above 70% the austenite grains became elongated parallel to the drawing direction. Depending on the used etchant, either grain boundaries or deformation bands were revealed. In the second case wide deformation bands were observed laying in two directions and crossing the whole sample (Fig. 6b and c).

Significant heterogeneity of the structure was found by TEM observations of thin foils (Fig. 7). Although both phases had lath morphology, small martensite areas could be found at the austenite bands (Fig. 7d). The TEM diffraction taken from areas with different dislocation density confirmed that there was the K-S relation between austenite and martensite adjacent areas (Fig. 7b).

4. Conclusions

Based on diffraction analysis, microstructure observations, magnetic and mechanical investigations the following conclusion could be formulated:

1. The multistage cold drawing of the austenitic stainless wires resulted in the occurrence of the strain induced $\gamma \rightarrow \alpha$ phase transformation.
2. When deformed, both phases (austenite and martensite) became textured. The austenite texture was typical for low SFE steels with two components <111> + <001>.
3. With the increasing deformation martensite texture was developed with two dominating components, i.e. the {hkl}<210> and {hkl}<110>.
4. The mutual relationships between austenite and martensite texture components were best described by K-S relation.
5. The deformation microstructure had fibre morphology with many shear bands which indicated at structure heterogeneity.
6. In the course of deformation, the volume fraction of martensite increased at the expense of the amount of austenite resulting in the hardening of the material.
7. In general a gradual increase of the yield strength results from both; the strain hardening of the austenite structure and formation of strain-induced martensite.

Acknowledgements

The work was supported by the Polish Committee for Scientific Research (KBN) under the contract No. 4.T08B.029.25.

REFERENCES

[1] F. B. Pickering, Rozwój metaloznawstwa stali odpornych na korozje, Hutnik 8/9, 343-365 (1978).

[2] Y. H. Park, Z. H. Lee, The effect of nitrogen and heat treatment on the microstructure and tensile properties of 25 Cr-7Ni-1.5Mo-3W-xN duplex stainless steel castings, Materials Science and Engineering **A 297**, 78-84 (2001).
[3] G. Balachandran, M. L. Bhatia, N. B. Ballal, P. Krishna Rao, Some Theoretical Aspects on Designing Nickel Free High Nitrogen Austenitic Stainless Steels, ISIJ International **41**, 9, 1018-1027 (2001).
[4] J. R. Davis ed, Alloy Digest Surcebook: Stainless Steels, 2000.
[5] A. Bunsch, W. Ratuszek, F. Ciura, K. Chruściel, Effect of Phase Transformation on the Austenite and Martensite Texture in Fe-30Ni Alloy, Archives of Metallurgy and Materials **50**, 2, 333-338 (2005).
[6] B. Ravi Kumar, A. K. Singh, S. Das, D. K. Bhattacharya, Cold Rolling in AISI 304 Stainless Steel, Materials Science and Engineering **A364**, 132-139 (2004).
[7] F. Borik, R. H. Richman, Preferred Transformations in Strain-Hardened Austenite, Transactions of the Metallurgical Society of AIME **239**, 675-680 (1967).
[8] W. Hübner, Phase Transformations in Austenitic Stainless Steels During Low Temperature Tribological Stressing, Tribology International **34**, 231-236 (2001).
[9] A. F. Padilha, P. R. Rios, Decomposition of Austenite in Austenitic Stainless Steels, ISIJ International **42**, 4, 325-337 (2002).
[10] J. C. Bavay, Les editions de physique, France 1993.
[11] B. Thomas, G. Henry, Les editions de physique, France 1993.
[12] J. Łuksza, M. Rumiński, W. Ratuszek, M. Blicharski, Badania mechanizmu zmian plastyczności w stali AISI 302 ciągnionej z bardzo dużymi odkształceniami, Hutnik 1-2, 53-58 (2007).
[13] J. Łuksza, M. Rumiński, W. Ratuszek, M. Blicharski, Texture evolution and variations of α-phase volume fraction in cold-rolled AISI 301 steel strip; Journal of Materials Processing Technology **177**, 555-560 (2006).
[14] H. Oettel, U. Martin, The nature of the TRIP-effect in metastable austenitic steels, Int. J. Mat. Res. (formerly Z. Metallkd.) **97**, 12 (2006).
[15] T. Angel, Formation of Martensite in Austenitic Stainless Steels Effect of Deformation, Temperature and Composition, Journal of the Iron and Steel Institute 165-174 (1954).
[16] D. Raabe, Texture and Microstructure Evolution During Cold Rolling of a Strip Cast and of Hot Rolled Austenitic Stainless Steel, Acta Materialia **45**, 3, 1137-1151 (1997).
[17] E. Nagy, V. Martinger, F. Tranata, J. Sólyom, Deformation Induced Martensitic Transformation in Stainless Steels, Materials Science and Engineering **A378**, 308-313 (2004).
[18] A. F. Padilha, R. L. Plaut, P. R. Rios, Annealing of Cold-Worked Austenitic Stainless, ISIJ International **43**, 2, 135-143 (2003).
[19] J. Karp, Praca doktorska, Rentgenowska ilościowa analiza fazowa drutów ze stali typu 18-9 wykazujących teksturę, AGH, Kraków (1960).

Received: 3 December 2007.